Pyroxene Europium Valence Oxybarometer. Effects of Pyroxene Composition, Melt Composition and Crystallization Kinetics. C. K. Shearer[1] , J.J. Papike[1] , and J. Karner[1]. [1]Institute of Meteoritics, Department of Earth and Planetary Science, University of New Mexico 87131 (cshearer@unm.edu),

Introduction: The behavior of multivalent elements such as iron, chromium, vanadium, and europium in magmatic systems reflects the f_{O2} of the environment. The oxidation state of these elements will influence the mineral assemblage, crystallization sequence, and element partitioning[1]. The effect of f_{O2} on the relative proportions of divalent and trivalent Eu has proven to be a useful tool for estimating f_{O2} in a variety of magmatic systems [e.g., 2,3]. The behavior of Eu in pyroxene from martian basalts has been demonstrated to be an effective measure of f_{O2} [e.g., 4,5]. These studies demonstrate both the power of Eu valence as an oxybarometer and its dependence on a number of magmatic and mineralogical variables. Here, we evaluate the effect of pyroxene and melt composition, crystallization sequence, and crystallization kinetics on the behavior Eu in natural basalts from similar, reducing environments (IW-1) of the Moon and the HED parent body (presumably 4 Vesta) and assess the influence of these variables on Eu valence as an oxybarometer.

Experimental Design and Analytical Approach: To compare Eu^{2+}/Eu^{3+} in lunar basalts and eucrites and to better understand the variables that may affect this indicator of f_{O2} in basalts, we selected two isochemical lunar pigeonite basalts (15058, 15499), a high-Ti lunar basalt (75035) and Pasamonte, an unequilibrated eucrite. All of these basalts crystallized at an f_{O2} of approximately IW-1. Yet, they all have different cooling histories, crystallization histories, and pyroxene compositional trajectories within the pyroxene quadrilateral. The two lunar pigeonite basalts have experienced different cooling and crystallization histories [6]. Basalt 15499 cooled at a rate of 5 to 20°C/hour, whereas 15058 cooled at a rate of < 1°C/hour [6]. The high-Ti lunar basalt and the basalt clasts in Pasamonte represent basalts that had intermediate cooling rates [6,7]. All pyroxenes were BSE imaged and compositionally mapped using scanning electron microscopy and electron microprobe. Imaging and major element analyses were used to strategically select a smaller subset of points for trace element ion microprobe analyses. A Cameca 4f ims at the Institute of Meteoritics (IOM), University of New Mexico was used to analyze Sm and Eu at all selected points. REE patterns (La, Ce, Nd, Sm, Eu, Dy, Er,, and Yb) were determined in a smaller subset of points.

Results: Major and minor element zoning characteristics of the pyroxenes in 15058, 15499, 75035, and Pasamonte are illustrated in Figures 1 and 2. Pyroxene from the Apollo 15 pigeonite basalts have two compositional trends observed on the pyroxene quadrilateral: a calcium enrichment trend with a variable discontinuity between pigeonite and augite normal to (110) of the pyroxene and a calcium-poor trend normal to (010). The Wo content of the pyroxene is related to the incoming of plagioclase in the crystallization sequence. Compared to the pyroxene in 15058, pyroxene in 15499 exhibits a slightly higher enrichment in calcium. Pyroxene in 15058 exhibits a much more striking iron-enrichment and a depletion in Ca once plagioclase is a liquidus phase. In 15058 approximately 50% of the pyroxene phenocryst crystallized prior to plagioclase crystallization, whereas in 15499 greater than 95% of the phenocryst crystallized prior to plagioclase. Compositional zoning in 75035 and Pasamonte are far less complex. Pyroxene in 75035 exhibits extreme iron-enrichment associated with Ca depletion from core to rim. In contrast, pyroxene from Pasamonte exhibits moderate iron-enrichment with an increase in calcium from pigeonite cores to augite rims.

Plagioclase crystallization affects minor element zoning in pyroxene. In the two pigeonite basalts, early pigeonite has low Si/Al and Ti/Al. With continued crystallization these two ratios increase until plagioclase becomes a liquidus phase. The increase in Si/Al generally reflects enrichment in melt in Al prior plagioclase saturation. Due to the difference cooling rate plagioclase crystallization in 15499 is delayed and results in extreme Al enrichments in the melt and pyroxene. Earlier plagioclase saturation in 15058 results in a dramatic decrease in Si/Al followed by a limited variation in this ratio with further iron-enrichment. In basalt 75035, the Si/Al ratio exhibits only an initial decrease followed by a limited variation in this ratio with further iron-enrichment. In Pasamonte, the earliest pigeonite has a somewhat varied Al (1.4 to 2.2 Al_2O_3) and the highest Si/Al and Ti/Al. The Si/Al decreases from core to rim.

In general, the low-Ca pyroxenes have a LREE depleted REE patterns. With increasing calcium in all of these pyroxenes, the LREE depletion is reduced and the overall REE abundance increases. This has been attributed to the affect of Ca substitution into the M2 site. With the iron-enrichment exhibited by pyroxene in several of the basalts, the REE pattern remains the same, yet the abundance increases. The relationship among Eu/Eu*, pyroxene composition, and onset of plagioclase crystallization is illustrated in

Figure 1 and 2. The behavior of Eu/Eu* in pyroxenes from 15058 is much more complex than the other basalts in this study. The Eu/Eu* decreases from approximately 0.44 to 0.30 with increasing Wo content in the pyroxene prior to plagioclase co-crystallizing with pyroxene. Once plagioclase becomes a liquidus phase, Eu/Eu* increases abruptly and then decreases to the Fe-rich pyroxene rim. In the more quickly cooled pigeonite basalt (15499), Eu/Eu* decreases more abruptly than in 15058 (0.46 to 0.22) with increasing Ca content of the pyroxene. The Eu/Eu* then remains constant in the rim of the pyroxene. The Eu/Eu* also appears to be different within different growth surfaces. For example, Eu/Eu* is greater in the sector normal to (110) than the sector normal to (010). In the basalt represented by 75035, as the total REE abundances increase from the pyroxene Mg-rich cores toward the Fe-rich rims, the Eu/Eu* decreases from approximately 0.42 to 0.20. In the pyroxene in Pasamonte, pyroxenes cores appear to have variable Eu/Eu* which appears to correlate with Al abundance. The Eu/Eu* decreases slightly and then remains fairly constants with increasing Ca and Fe.

Discussion: There are several variable that influence the Eu/Eu* recorded in pyroxene that may compromise the determination of f_{O2}. Previous experimental studies show that pyroxene composition influences the ability of pyroxene to accommodate REE and fractionate Eu^{2+} from Eu^{3+}. We demonstrate that in addition to the influence of Ca in the M2 site, the Al content in the pyroxene and its influence on coupled substitutions will also influence the fractionation of Eu^{2+} from Eu^{3+}. For example, the coupled substitution Si^{4+} (T) + R^{2+} (M2) $\Rightarrow$ Al^{3+} (T) + REE^{3+} (M2) may accommodate REE^{3+} in preference to Eu^{2+} which is too large. Different pyroxene growth surfaces will incorporate Eu^{2+} and Eu^{3+} differently due to differences in growth rate and site configuration. In consort with the pyroxene composition, fractionation of Eu^{2+} from Eu^{3+} will be aided by the Al content of the basaltic melt which increases the activities of the network-forming components such as $CaAl_2O_4$ and $FeAl_2O_4$ in the melt during pyroxene crystallization. Melt composition, the appearance of plagioclase on the liquidus and the kinetics of plagioclase crystallization are influenced by cooling rate. The four basalts selected also suggest that Eu^{2+}/Eu^{3+} in the melt remains buffered even with some of the extreme differences in cooling rate and plagioclase crystallization kinetics. Many of these same variables affect the substitution of multivalent V. If the f_{O2} determined from Eu behavior in pyroxene is not placed within a petrologic and crystal chemical context errors of 1 to 2 log units may result. The influence of these variables may be reduced by using multiple, co-crystallizing phases (i.e. plagioclase and pyroxene) and ratioing D_{Eu} to adjacent REE ($D_{Sm, Gd}$).

References: [1] Papike et al. (2005) Am. Min. 90, 277-290. [2] Philpotts, J.A. (1970)*EPSL* 9, 257-268. [3] McKay, G.A. et al.(1994) *Proc. 25th LPSC* 883-884. [4] Wadhwa, M. (2001) *Science* 291, 1527-1530. [5] McCanta, M.C. and Rutherford, M.J. (2002) In *Unmixing the SNCs*. LPI Contribution 1134. Houston: Lunar and Planetary Institute, p. 35. [6] Bence, A.E. and Papike, J.J. (1972) *Proc. 3rd LSC* 431-469. [7] BVSP (1981) Basaltic volcanism on the terrestrial planets. Pergamon Press, New York, 1286.

Figure 1. Pyroxene quadrilateral and Eu/Eu* for pyroxene.

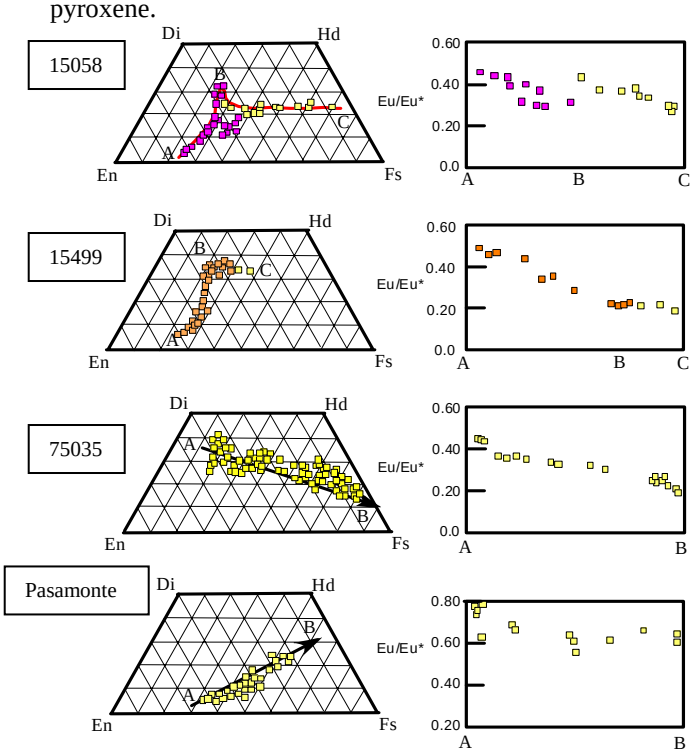

Figure 2. Al/Si versus Fe/Mg for pyroxenes used in this study.